

1

2

Supporting Information

3 **1. Apparatus**

4 Transmission electron microscopy (TEM) of obtained nanocomposites was
5 performed by G2 F20 S-TWIN transmission electron microscope for the
6 morphologies investigation. X-ray photoelectron spectroscopy (XPS) was determined
7 via AXIS Ultra DLD electron spectrometer (Kratos) to confirm the elemental
8 composites of PPy nanoparticles and PPy@MnO₂ nanocomposites. The chemical
9 component and structure of products was further evaluated by Fourier transform
10 infrared spectra (FT-IR) using TENSOR II (Bruker, Germany). The dynamic light
11 scattering (DLS) data and Zeta potential were measured by using Zetasizer Nano ZS
12 (UK) to obtain average hydrodynamic particle sizes and polydispersity index (PDI)
13 values, and monitor the construction process of products, respectively.
14 Thermogravimetric analysis (TGA) was obtained by TGA Q50 thermo-gravimetric
15 analyzer (TA Instruments, USA) under nitrogen atmosphere with a heating rate of 20
16 °C min⁻¹. U-2910 Spectrophotometer (Hitachi, Japan) was utilized to collect UV-vis
17 spectrum, and UV-vis-NIR spectra was harvested via Lambda 950 UV-vis-NIR
18 spectrophotometer (PerkinElmer, USA). Confocal laser scanning microscopy (CLSM)
19 was obtained by Zeiss LSM-880 (Carl Zeiss, Germany).

20 **2. Synthesis of core polypyrrole nanoparticles (PPy NPs)**

21 1.6 g PVA (Mw: 13000-23000) were dissolved into 20 ml deionized water and 1.2
22 g FeCl₃·6H₂O were added, then stirred for 1 h. Subsequently, 140 μL of pyrrole
23 monomer were dropped into the above solution. After stirring continuously for 4 h at
24 4 °C, the product was harvested by centrifugation and washed several times with hot
25 deionized water to remove unreacted PVA. Finally, the product was freeze-dried to
26 afford a fine black powder of PPy nanoparticles.

27 **3. Detection of extracellular ¹O₂ and intracellular ROS generation**

28 To explore the effect of pH on extracellular ¹O₂ generation, 15 μL DPBF solution

1 (10 mM in DMSO) were added to 2 mL PBS-ethanol mixed solution (pH 7.4) of 20
2 $\mu\text{g}/\text{mL}$ PPy@MnO₂-PEG-MB nanocomposites. After the addition of 100 μM H₂O₂,
3 the mixture was illuminated with 635 nm laser (10 min, 50 mW·cm⁻²) under dark. The
4 UV-vis absorption intensity of DPBF at 410 nm was measured every 2 min. And the
5 group without laser was set as a control. The generation of ¹O₂ in others pH were
6 measured by a similar method, only replace the PBS (pH 7.4) with the PBS (pH 5.0 or
7 6.0) to imitate cancer acidic microenvironment.

8 For intracellular ROS, HeLa cells were seeded in a six-well culture plate for 24 h,
9 then treated with 200 $\mu\text{g}/\text{mL}$ of PPy@MnO₂-PEG-MB nanocomposites or 70.2 $\mu\text{g}/\text{mL}$
10 of MB for 4 h. After rinsing the cells with PBS solution for three times, 100 μL
11 DCFH-DA (10 $\mu\text{mol}/\text{L}$) were added and treated for 30 min. Then the cells were
12 washed with PBS solution for two times to remove excess DCFH-DA. Finally, the
13 cells were exposed to 635 nm laser (10 min, 50 mW·cm⁻²). The cells without added
14 particles were used as a control. The generation of intracellular ROS was captured by
15 confocal laser scanning microscopy (CLSM) under 488 nm excitation and 510-560
16 nm emission.

17 **4. Detection of extracellular stability of PPy@MnO₂-PEG-MB** 18 **nanocomposites and the release of MB from the nanocomposites**

19 The stability of PPy@MnO₂-PEG-MB nanocomposites in different conditions were
20 studied by monitoring amount of retained MnO₂ through UV-vis absorption
21 intensities. The different pH values (7.4, 5.0) of phosphate-buffered saline (PBS)
22 solutions in the presence/absence of 0.25/100 μM H₂O₂ containing PPy@MnO₂-PEG-
23 MB nanocomposites were shaking at 37 °C. At different time intervals, a small
24 amount of solution was removed for measuring the UV-vis absorption spectra, such as
25 0.25, 0.5, 1, 2, 3, 4, 5, 12 and 24 h.

26 Then the release behaviors of MB from PPy@MnO₂-PEG-MB nanocomposites in
27 different conditions were detected. In a dark environment, 200 $\mu\text{g}/\text{mL}$ of PPy@MnO₂-
28 PEG-MB nanocomposites were transferred to a dialysis bag (MWCO: 3500), then
29 placing the dialysis bags in different media, such as PBS solutions of pH 7.4 in the

1 presence/absence of 0.25 μM H_2O_2 and pH 5.0 in the presence/absence of 100 μM
2 H_2O_2 , respectively. After shaking at 37 $^\circ\text{C}$ for various time intervals (0.5, 1, 2, 3, 4, 5,
3 6, 12 and 24 h), 2 mL of media were taken out and replaced with equal volume fresh
4 media. The liberated MB concentrations were finally calculated by UV-vis absorption
5 intensities of removed solutions based on standard MB curve.

6 **5. Cellular uptake and photothermal/photodynamic therapy assays**

7 For cellular uptake assays, HeLa cells were seeded in a six-well culture plate. After
8 incubation overnight, the culture medium was removed and 200 $\mu\text{g}/\text{mL}$ of
9 PPy@MnO₂-PEG-MB nanocomposites or 70.2 $\mu\text{g}/\text{mL}$ of MB were added. After 4 h,
10 the cells were rinsed with PBS to the extracellular nanocomposites. The cells without
11 treated were set as a control. The fluorescence images were monitored by CLSM. The
12 lysosomal localization experiment of PPy@MnO₂-PEG-MB nanocomposites in HeLa
13 cells was carried out using similar method. The green commercial lysosomal tracker
14 was added and incubated for 30 min after the cells treated with nanocomposites for 4
15 h. The CLSM was also applied to obtain fluorescence images with green and red dual-
16 channels.

17 To explore the biocompatibility of nanocomposites, HeLa cells were cultured in a
18 96-well plate in Dulbecco's modified Eagle's medium (DMEM) containing 10% fetal
19 bovine serum (FBS), 50 mg/mL penicillin, and 50 mg/mL streptomycin at 37 $^\circ\text{C}$ and
20 5% CO_2 . After incubation for 24 h, different concentrations of PPy nanoparticles,
21 PPy@MnO₂-PEG nanocomposites and PPy@MnO₂-PEG-MB nanocomposites in
22 culture medium were introduced to each well and the cells were cultured for another
23 12 h. MTT solution was added into each well and incubated for further 4 h. Then, an
24 enzyme-linked immunosorbent assay (ELISA) reader was used to determine the
25 absorbance of suspension.

26 To assess the in vitro photothermal/photodynamic therapy (PTT/PDT) effect of
27 PPy@MnO₂-PEG-MB nanocomposites, HeLa cells were seeded in a 96-well culture
28 plate for 24 h, then the cells were treated with PPy@MnO₂-PEG-MB nanocomposites
29 possessing various concentrations for 4 h. Then for single PTT or PDT group, the

1 cells were irradiated with the 808 nm laser ($2 \text{ W}\cdot\text{cm}^{-2}$, 5 min) or exposed to the 635
 2 nm laser ($50 \text{ mW}\cdot\text{cm}^{-2}$, 5 min), while for combined therapy group, the cells were first
 3 irradiated by the 808 nm laser ($2 \text{ W}\cdot\text{cm}^{-2}$, 5 min) and then dealt with the 635 nm laser
 4 ($50 \text{ mW}\cdot\text{cm}^{-2}$, 5 min). The cells without irradiated were served as a control. After
 5 cultured for further 8 h, the cell viability was observed by MTT assay.

6 6. Calculation of photothermal conversion efficiency

7 The photothermal conversion efficiency (η) of nanomaterials could be calculated
 8 according to reported method[1]. The details of calculation of photothermal
 9 conversion efficiency were as follows:

$$\eta = \frac{hA(\Delta T_{max,mix} - \Delta T_{max,H_2O})}{I(1 - 10^{-A_{808}})} \quad (1)$$

10 where h is the heat transfer coefficient, A is the surface area of the container. $\Delta T_{max,mix}$
 11 and $\Delta T_{max,H_2O}$ are the temperature variations of nanomaterials solution and deionized
 12 water after laser radiation. I refers to the laser power and A_{808} is the absorbance of
 13 nanomaterials at 808 nm.

14 Then the value of hA was calculated from equation (2):

$$hA = \frac{m_{H_2O}C_{p,H_2O}}{\tau_s} \quad (2)$$

15 where m_{H_2O} and C_{p,H_2O} refer to the mass and heat capacity of deionized water,
 16 separately. τ_s is a sample system time constant.

17 The value of τ_s was obtained from equation (3) and (4):

$$\theta = \frac{(T - T_{surr})}{(T_{max} - T_{surr})} \quad (3)$$

$$t = -\tau_s \ln \theta \quad (4)$$

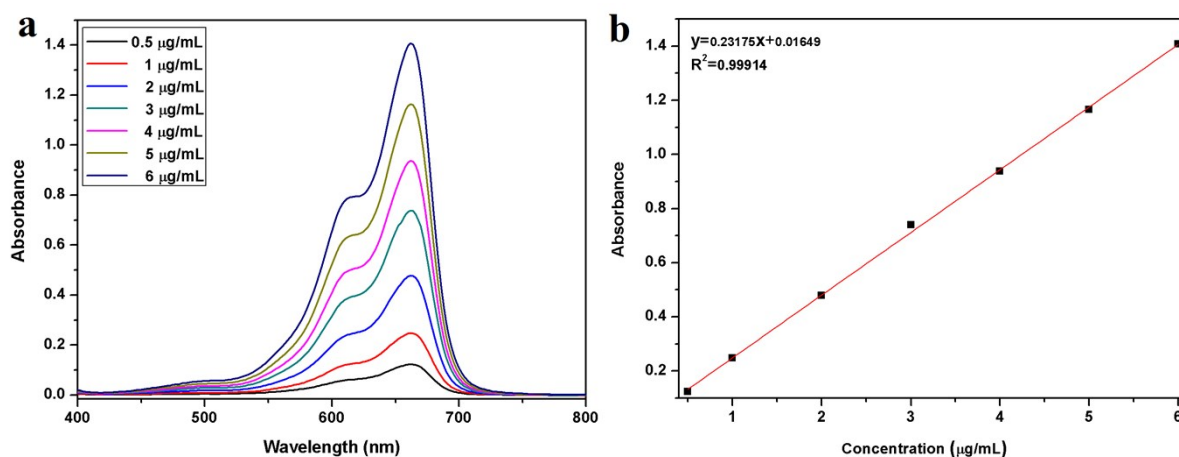
18 where θ is a dimensionless parameter, T refers the temperature during natural cooling
 19 stage. T_{surr} is the environment temperature and T_{max} is the maximum steady
 20 temperature. Therefore, τ_s is able to determine.

21 Finally, substituting our corresponding value into equation (1), the photothermal

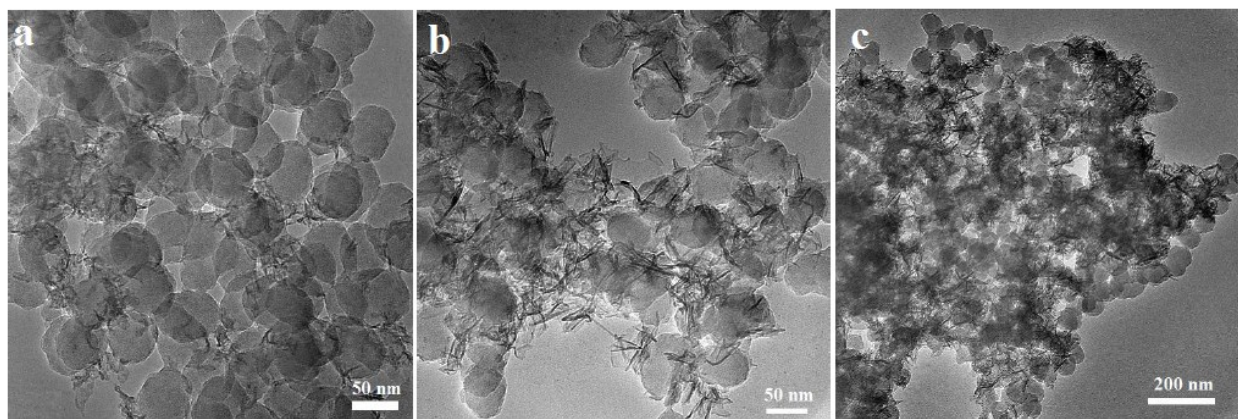
1 conversion efficiency (η) of PPy@MnO₂-PEG-MB nanocomposites was assessed to
2 be 54.4%.

3 References

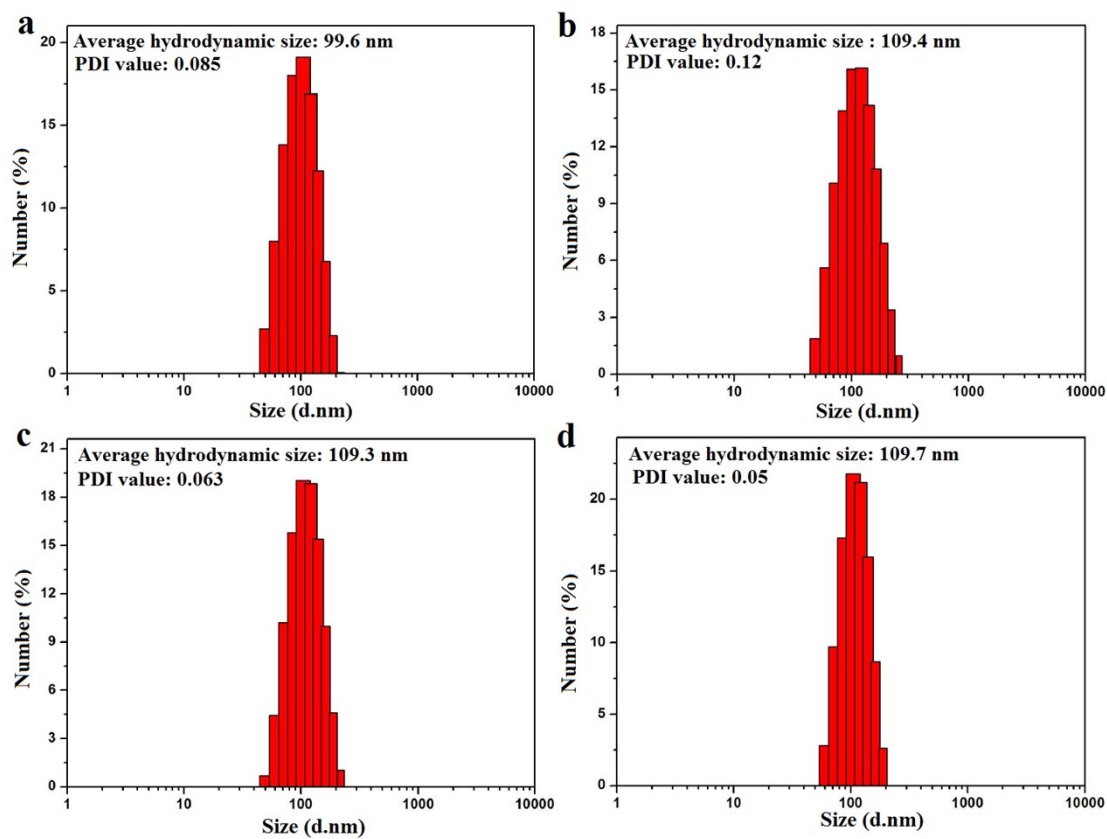
4 [1] W. Ren, Y. Yan, L. Zeng, Z. Shi, A. Gong, P. Schaaf, D. Wang, J.
5 Zhao, B. Zou, H. Yu, G. Chen, E. M. B. Brown, and A. Wu, A near
6 infrared light triggered hydrogenated black TiO₂ for cancer
7 photothermal therapy, Adv. Healthcare Mater., 2015, 4, 1526–1536.



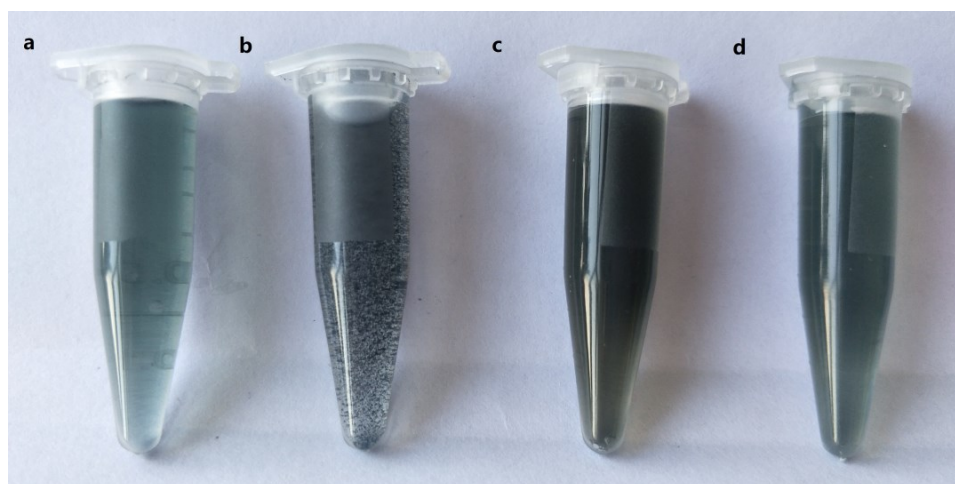
8
9 Figure S1. (a) UV-vis spectrums of MB with different concentrations, (b) the standard curve of
10 MB.



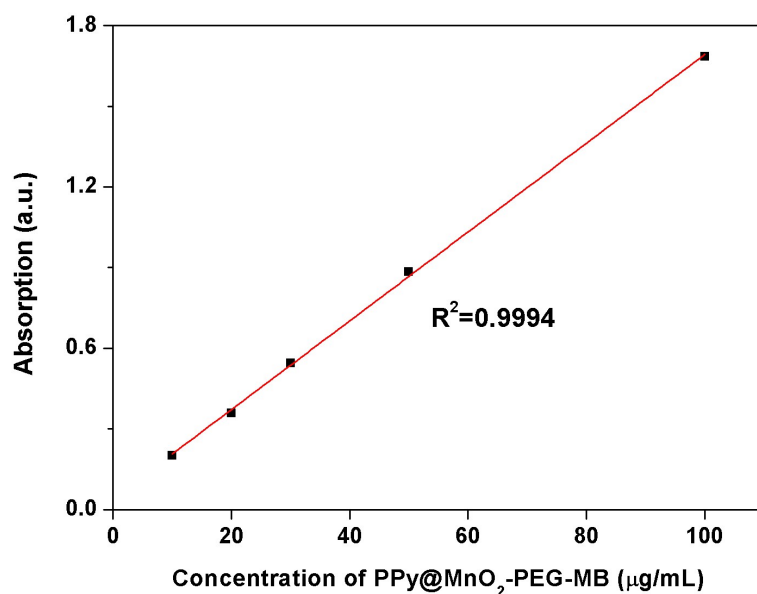
11
12 Figure S2. TEM images of PPy@MnO₂ nanocomposites under different mass ratios of KMnO₄ to
13 PPy nanoparticles. (a) 0.5:1, (b) 1:1 and (c) 2:1.



1
 2 Figure S3. Size distributions of (a) PPy nanoparticles, (b) PPy@MnO₂, (c) PPy@MnO₂-PEG, (d)
 3 PPy@MnO₂-PEG-MB nanocomposites by dynamic light scattering (DLS) tests.



4
 5 Figure S4. Photos of (a) PPy nanoparticles, (b) PPy@MnO₂, (c) PPy@MnO₂-PEG, (d)
 6 PPy@MnO₂-PEG-MB nanocomposites.

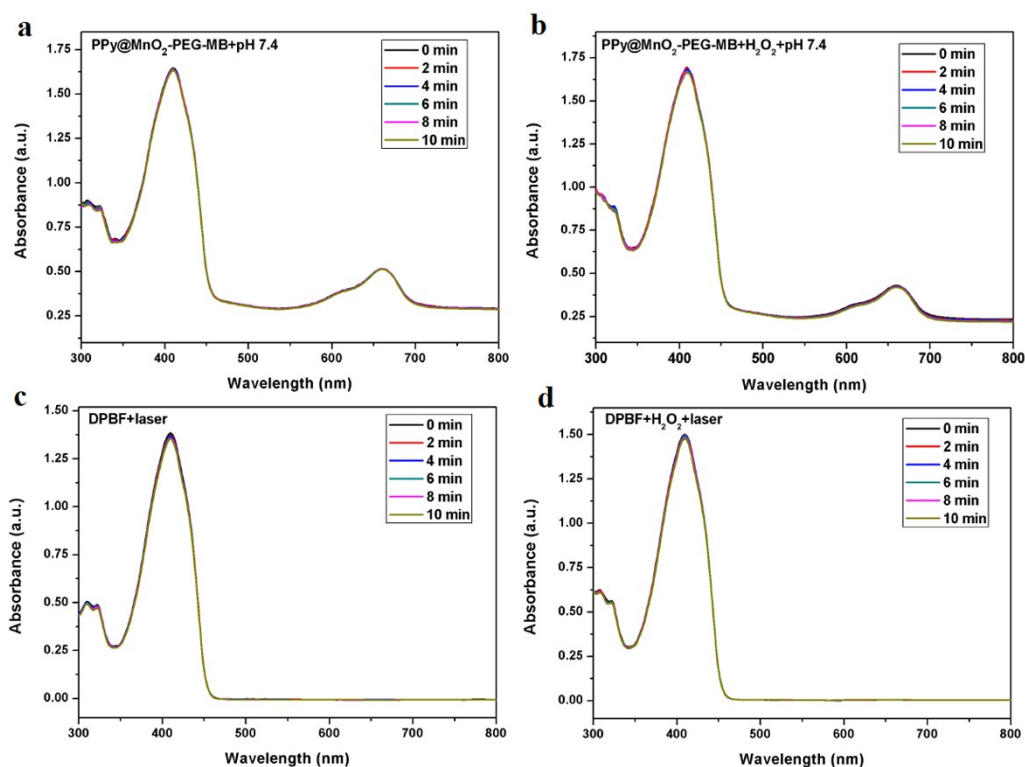


1

2 Figure S5. Linear fitting of the absorbance of PPy@MnO₂-PEG-MB nanocomposites at 808 nm

3

versus the nanocomposites concentrations.



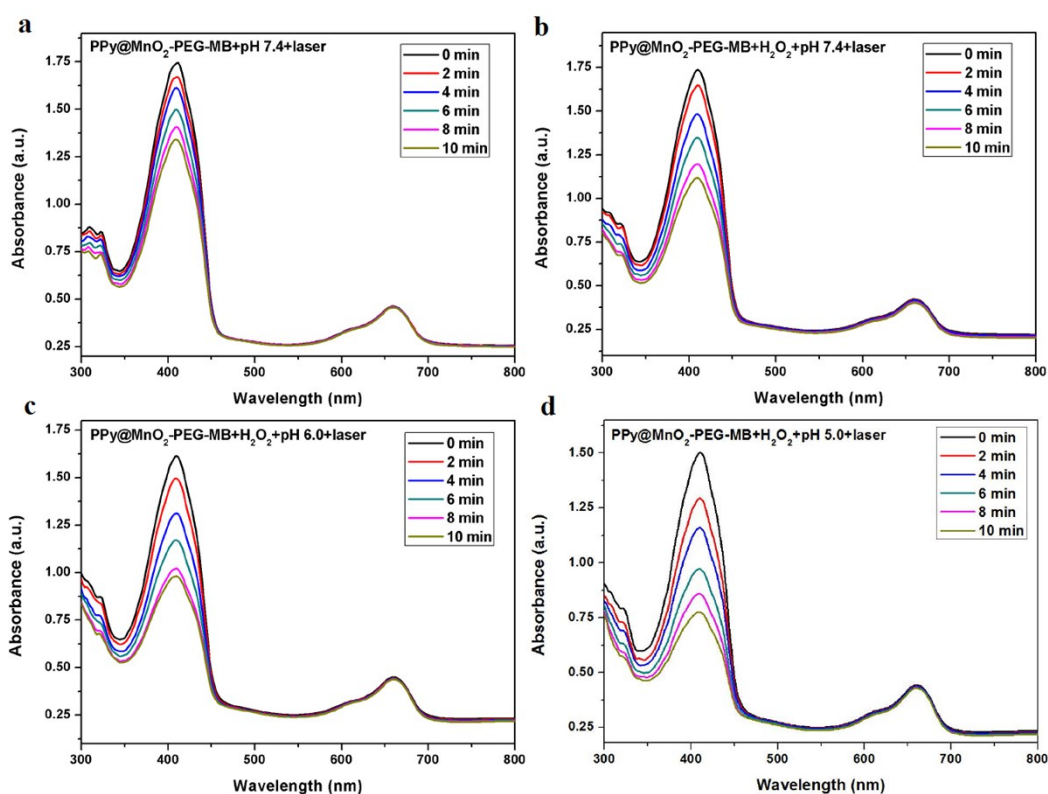
4

5 Figure S6. UV-vis spectrums of DPBF under different conditions, PPy@MnO₂-PEG-MB (pH

6 7.4), PPy@MnO₂-PEG-MB+H₂O₂ (pH 7.4) without laser (10 min), DPBF only and DPBF+H₂O₂

7

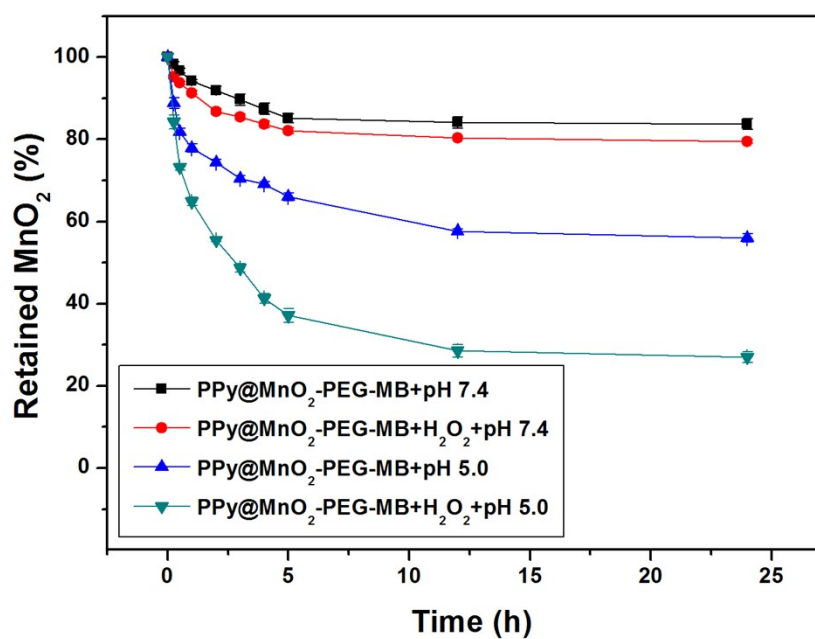
with 635 nm laser (10 min).



1

2 Figure S7. UV-vis spectrums of DPBF under various conditions, PPy@MnO₂-PEG-MB (pH 7.4),

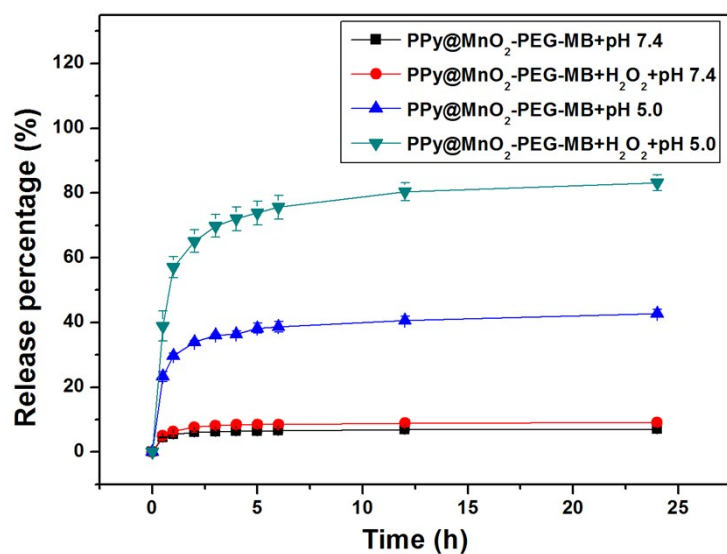
3 PPy@MnO₂-PEG-MB+H₂O₂ at various pH values (7.4, 6.0, 5.0) with 635 nm laser for 10 min.



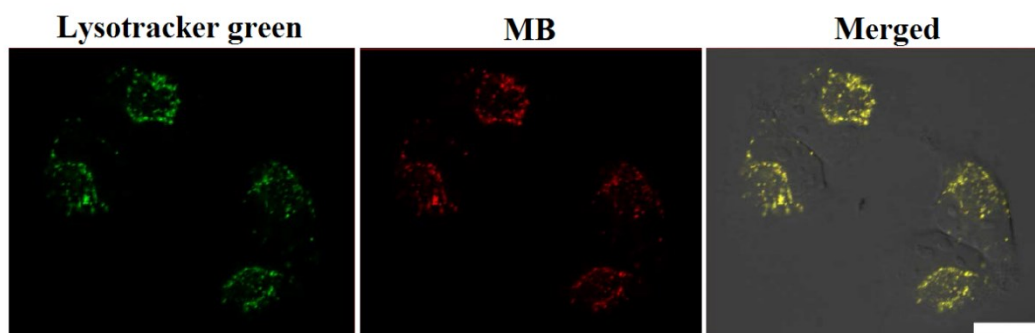
4

5 Figure S8. The degradation abilities of PPy@MnO₂-PEG-MB at different pH values (7.4, 5.0) in

6 the presence/absence of H₂O₂ at 37 °C. Error bars were based on triplicate experiments.



1
 2 Figure S9. The MB release profiles from PPy@MnO₂-PEG-MB at different pH values (7.4, 5.0) in
 3 the presence/absence of H₂O₂ at 37 °C. Error bars were based on triplicate experiments.



4
 5 Figure S10. The confocal images of HeLa cells treated with PPy@MnO₂-PEG-MB
 6 nanocomposites and lysosomal tracker green. Scale bar: 20 μm.